Signatures of single-photon interaction between two quantum dots located in different cavities of a weakly coupled double microdisk structure

S. Seyfferle,[1] F. Hargart,[1] M. Jetter,[1] E. Hu,[2] and P. Michler[1]

[1]*Institut für Halbleiteroptik und Funktionelle Grenzflächen, Research Center SCoPE and IQST, Universität Stuttgart, Allmandring 3, 70569 Stuttgart, Germany*

[2]*School of Engineering and Applied Sciences, Harvard University, 29 Oxford Street, Cambridge, Massachusetts 02138, USA*

(Received 28 September 2017; revised manuscript received 15 December 2017; published 9 January 2018)

We report on the radiative interaction of two single quantum dots (QDs) each in a separate InP/GaInP-based microdisk cavity via resonant whispering gallery modes. The investigations are based on as-fabricated coupled disk modes. We apply optical spectroscopy involving a $4f$ setup, as well as mode-selective real-space imaging and photoluminescence mapping to discern single QDs coupled to a resonant microdisk mode. Excitation of one disk of the double cavity structure and detecting photoluminescence from the other yields proof of single-photon emission of a QD excited by incoherent energy transfer from one disk to the other via a mode in the weak-coupling regime. Finally, we present evidence of photons emitted by a QD in one disk that are transferred to the other disk by a resonant mode and are subsequently resonantly scattered by another QD.

DOI: 10.1103/PhysRevB.97.035302

I. INTRODUCTION

The scientific development towards quantum technologies based on semiconductor solid-state devices has seen much progress in recent years. In particular, semiconductor quantum dots (QDs) put themselves forward for the implementation as qubits [1,2]. The coherent control of the interaction of two QDs in coupled quantum systems is a key element and promises, e.g., the implementation of parallel qubit operation for quantum information processing. To this end, Imamoğlu *et al.* proposed [3] to utilize two spatially distant electron spins of QD excitons inside a microcavity coupled by a single cavity field to implement CNOT operations.

The coupling of two QDs in one cavity has been realized in micropillar [4] and photonic crystal cavities [5,6]. However, accomplishing selective tunability and individual addressability of each QD, which is essential for the manipulation of individual qubits in future applications, is technically challenging for closely spaced QDs. Consequently, the idea is to exploit the long-range interaction between QDs in coupled microcavity systems, i.e., photonic molecules (PMs) [7–10] where the energy transfer is mediated via a resonant cavity mode. It has been shown recently that the excitation of a two-level system with quantum light instead of classical light could improve the quality of subsequently emitted single photons [11]. Thus, classical light could be used to excite a first QD which in turn excites a second QD with a stream of single photons. Using PMs to obtain an efficient coupling between the QDs presents an integrable and compact semiconductor solution. In addition, these PMs have also been theoretically investigated for entanglement of a pair of QDs [12,13], they enable the unconventional photon blockade [14,15], and serve as a starting point for the realization of driven-dissipative multicavity systems [16] and strong photon-photon correlations [17–19].

An attractive type of cavity system are the whispering gallery mode (WGM) supporting microdisks [see exemplary scanning electron microscope (SEM) picture in Fig. 1(a)]. The WGMs propagate along the inner edge of the disk and couple to an adjacent microdisk cavity via the exponentially decaying evanescent mode field outside of the disk slab. The concentration of the electromagnetic mode field along the rim of the disks grants an effective photonic coupling to the QDs. The WGMs are found to be TE and TM polarized but since the electric-field vector of the TE modes oscillates in the disk plane these modes preferentially couple to the in-plane QD dipole [20]. Furthermore, the micrometer dimensions of the cavity allow for convenient optical addressability of each microdisk.

In this paper, we present resonant scattering of single photons by a QD, which have been emitted by another QD in the other disk of the double GaInP-based microdisk structure containing an embedded active layer of InP QDs. The radiative excitation transfer is mediated by a weakly coupled cavity mode. The WGM wavelength is very sensitive to the disk diameter leading to a mode energy mismatch between the disks because of imperfections in the fabrication process. These spectral mode differences can be compensated by local tuning techniques, e.g., laser heating [21,22], electrothermal heating [23], photoreactive materials [24], which are all based on the local control of the refractive index, or photoelectrochemical etching [25] to change the cavity dimension on the nanometer scale. However, most tuning techniques are experimentally very challenging or prevent single QD experiments, e.g., by high excitation powers necessary for sufficient cavity mode tuning. For that reason we follow a different approach by discerning modes which display evidence of resonance as fabricated, in order to be independent of tuning mechanisms. We identify possibly resonant microdisk modes by means of microphotoluminescene (μ-PL) spectroscopy scans in combination with real-space imaging, verify single-photon emission from QDs excited by energy transfer via mode coupling, and present indications of on-chip resonant scattering.

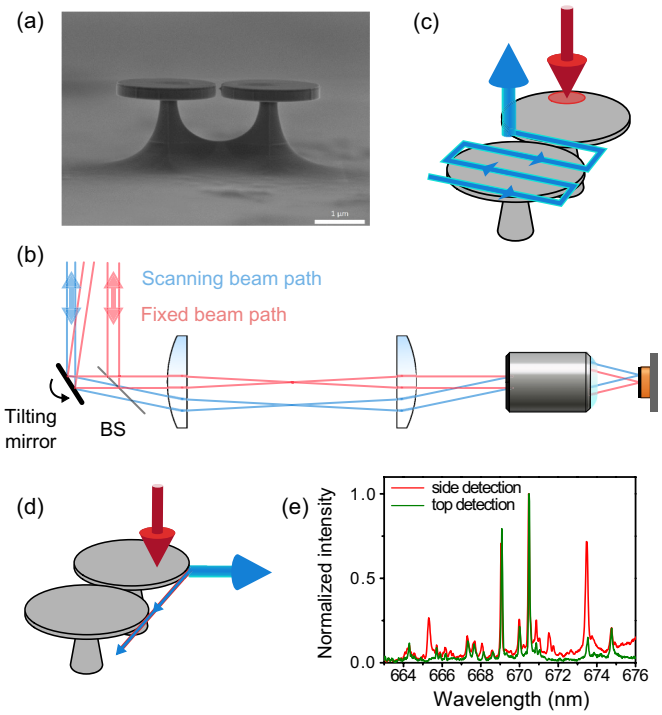

FIG. 1. (a) Exemplary SEM image of a microdisk dimer with a nominal interdisk spacing of 50 nm. (b) $4f$ setup for PL scans and maps. The lens configuration in combination with a piezo driven tiltable mirror enables us to scan detection and excitation independently from each other over the disk pair. (c) Schematic of the PL map scanning procedure, here, for fixed excitation (red) and scanning detection (blue). The setup also allows for other configurations, i.e., scanning both the excitation and detection, or fixed detection and scanning excitation. (d) Schematic of the PL side scanning procedure. The cryostat geometry makes it possible to optically access the sample also in plane. (e) Comparison of spectra taken from the disk side (red solid line) and disk top (green solid line).

II. SAMPLE AND SETUP

The sample exclusively studied in the work at hand was grown by metal-organic vapor-phase epitaxy (MOVPE). The microdisk post is made of $Al_{0.5}Ga_{0.5}As$:Si. The disk features layers of GaInP and AlGaInP symmetrically arranged around the active layer of InP QDs that have a density of 1.5×10^{10} cm^{-2}. The actual disk structure is finally formed by a combination of e-beam lithography, dry etching, and wet undercut etching. Fabrication and processing steps are detailed elsewhere [22]. The disk dimers have a nominal interdisk minimum edge separation of 50 nm while each disk possesses a diameter of 5 μm. Typical Q factors of the sample range in the order of 12 000. High Q factors are desirable to grant an efficient QD-mode coupling. In the so-called strong-coupling regime a coherent and reversible exchange of photons between QD and cavity mode is given which outweighs the cavity losses [26,27].

However, the following investigations are based on the weak coupling of both, QD to a mode as well as the coupling of two modes in different cavities. An estimate of the upper limit of the Purcell factor for a QD coupled to a disk mode based on the above mentioned Q factor and an exemplarily calculated mode volume of $V_{\mathrm{mode}} \approx 17(\lambda/n)^3$ can be given by $F_{\mathrm{P}} \approx 54$. Furthermore, the coupling strength can be estimated to $g \approx 62$ μeV using [28]

$$\frac{g}{2\pi} = \frac{1}{2\tau}\sqrt{\frac{3c\lambda^2\tau}{2\pi n^3 V_{\mathrm{mode}}}} \tag{1}$$

with a typical radiative lifetime of InP QDs of $\tau = 350$ ps [29] and a refractive index of the GaInP resonator of $n \approx 3.6$. Comparing g to the loss rate $\kappa = \omega/Q \approx 153$ μeV confirms that the system is in the weak-coupling regime. In this regime medium Q factors benefit the mode-mode coupling [10,21,22] between two different microdisks since a larger fraction of photons escape the cavity to interact with a resonant mode in the other. Therefore, also in the weak-coupling regime resonant energy transfer via cavity modes and dot-to-dot interaction is possible.

For the spectral characterization of the microdisks via μ-PL spectroscopy, the sample is placed inside a helium flow cryostat on a motorized stage at a nominal temperature of 4 K. The above band (532 nm) excitation laser (unpolarized white light supercontinuum system) applying a power below saturation is focused onto the outer disk rim through a 100x microscope objective (NA = 0.7). The focused spot diameter is estimated to <1.5 μm, thus largely excluding the possibility of involuntary excitation of QDs in the other disk, assuming a Gaussian laser intensity profile. The PL of the disks is collected by the same objective and passes through a $4f$ lens system of which a sketch is shown in Fig. 1(b). This top detection scheme mainly collects stray light of the mode emission since the modes emit predominantly radially and in plane. The $4f$ setup involving two convex lenses ($f = 20$ cm) and a piezo driven tiltable mirror allows for the spatial disconnection of excitation and detection beam paths in a confocal microscopy setup. This configuration makes possible either local invariant excitation of one disk of the dimer while simultaneously and independently scanning the detection across the complete disk pair by tilting the piezo mirror, or alternatively, moving the excitation spot while using a fixed detection spot. In this way, the whole disk pair can be scanned by stepwise movement of the tiltable mirror and recording a spectrum for each mirror position, as is schematically drawn in Fig. 1(c). This enables us to record one-dimensional scans as well as two-dimensional photoluminescence maps. The cryostat geometry also enables us to optically access and scan the sample from the side [see schematic Fig. 1(d)] thereby detecting mainly the in-plane mode emission.

For the purpose of real-space imaging using a charge-coupled device (CCD) the PL signal from the sample is collected by the same objective and focused via a collective lens onto a liquid-nitrogen-cooled CCD chip. Insertion of suitable bandpass filters enables us to image and identify only certain modes of interest by the presence of a ring of emission along the disk edge while dots appear as bright spots of high intensity.

A basic optical characterization of a disk pair is shown in Fig. 1(e). Spectra detected from the top of the disks (perpendicular to the sample surface, green solid line) and from the disk sides (in-plane, red solid line) are plotted for comparison. The

disk has been excited from the top and the spectra have been obtained by directly switching between the two orthogonal detection configurations without varying the setup further. The spectra show several sharp and bright emission lines likely due to high-Q modes fed by QDs interspersed with weaker and broader lines probably caused by modes of lower Q factor. Due to the predominant radial and in-plane emission characteristics of the WGM, it is expected to directly access mode emission from the side while only detecting mode stray light from the top. The two dominating lines at 669 and 670.4 nm appear almost equally bright in both detection schemes, whereas the peak at 673.5 nm displays higher intensity detected from the side. Consequently stray light collection for this mode from the top is less efficient. Additionally, there are two lines at 665.3 and 671.5 nm which only appear in the side detection and can be assumed to be disk modes whose stray light is not scattered into the top microscope objective. The overall similar appearance of the two spectra shows that stray-light detection from the top is a convenient way for the optical investigations of the microdisk pairs especially with respect to imaging and mapping the mode profile from the top seen in the following.

III. IMAGING OF COUPLED AND UNCOUPLED MODES

Taking one-dimensional μ-PL spectroscopy scans as a starting point enables us to preselect possibly coupled disk modes by the observation of emission lines that display a considerable intensity at the same wavelength in both disks.

Figure 2(a) shows the scan of a dimer displaying a number of emission lines whose spatial distribution clearly outlines the individual disk location. The scan was obtained by stepwise motion of the above band excitation laser with an excitation power of 60 nW over the length of the dimer while acquiring a spectrum at each laser position.

Some emission lines can be seen to be situated at the same wavelength in both disks, which can be taken as a first hint at resonant modes, which in turn is a precondition for radiative interaction. Such a candidate is evident at 669 nm. A counterexample can be found at 666 nm where the intensity of the emission line is predominantly restricted to the disk in the bottom scan part. Both the presumably coupled (669 nm) and uncoupled mode (666 nm) have been selected for further investigations by real-space imaging [cf. Figs. 2(b)–2(e)]. The respective modes have been selected with an appropriate bandpass filter (transmission window ± 0.5 nm). The images in Figs. 2(b) and 2(c) have been recorded with the excitation laser fixed on the far edge of the bottom disk (see schematic insets in Fig. 2). In the case of the presumably uncoupled mode at 666 nm the lower disk reveals distinct centers of emission along the expected circular mode profile [Fig. 2(b)], whereas the upper disk does not contribute substantial PL, which supports the assumption that this mode has no resonant counterpart in the other disk. However, a ring of PL emission outlining the disk shape can be perceived in Fig. 2(c) in the case of the mode at 669 nm presumably tuned into resonance with a mode in the other disk. This indicates radiative excitation transfer from the excited disk to the nonexcited disk.

A cross check has been performed by placing the laser spot on the other disk [Figs. 2(d) and 2(e)]. Again, the nonexcited disk remains dark for the detuned mode at 666 nm [Fig. 2(d)],

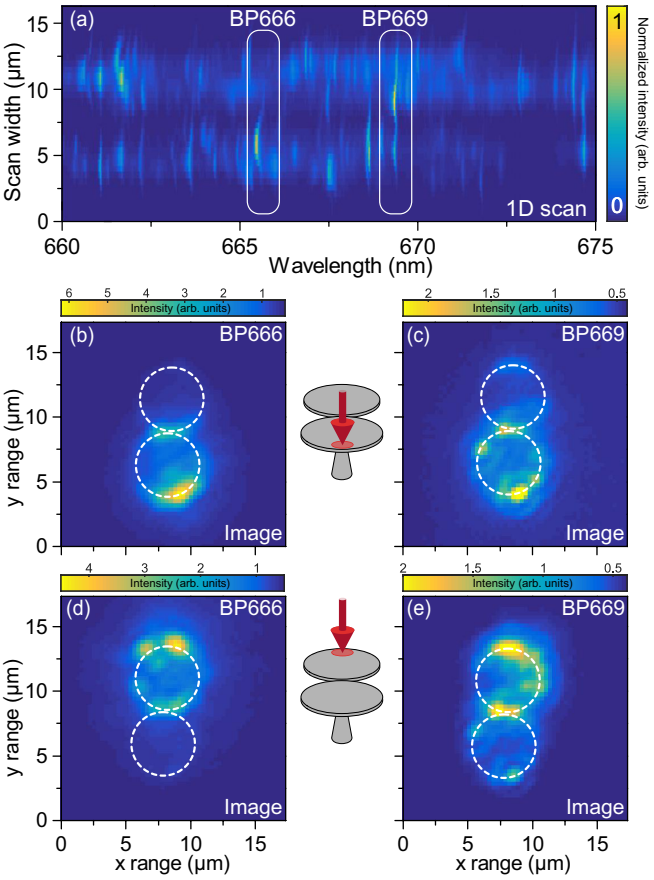

FIG. 2. (a) Normalized color-scale plot of a one-dimensional scan displaying emission lines from both disks. Two emission lines signified in the plot are selected for further investigations: a presumably coupled mode at ≈669 nm and an uncoupled mode at ≈666 nm. The emission lines display a slight wavelength shift. This is probably due to an artefact as the angle of incidence with respect to the spectrometer slit changes as the position is varied on the sample. (b)–(e) Real-space images of the disk pair evaluated with a bandpass filter at 669 nm (666 nm) for the (un)coupled mode. The lower disk is excited in (b) and (c) (see inset). Only in the case of the supposedly coupled mode does the nonexcited disk contribute PL. In the CCD images of (d) and (e) the upper disk is excited. Again, the nonexcited disk remains dark for the uncoupled mode. The red arrows in the insets show the spatial position of the excitation laser on the disk.

i.e., no excitation transfer from one disk to the other takes place. Note that in both disks QDs are present that emit around a wavelength of 666 nm, but only as a consequence of direct optical excitation by the laser. This observation should exclude other excitation transfer processes, e.g., via phonons or scattering processes. The same procedure has been carried out for the presumably coupled mode [Fig. 2(e)]. The nonexcited lower disk is clearly visible by a ring of emission along the disk edge where the mode is expected to propagate, as well as bright circular centers of high intensity which indicate QDs excited by transferred light. Another feature that appears in the images of Figs. 2(c) and 2(e) is a striking bright luminescence at the interdisk gap. A possible preliminary explanation might be the presence of an enhancement of the electric field at the contact point [30].

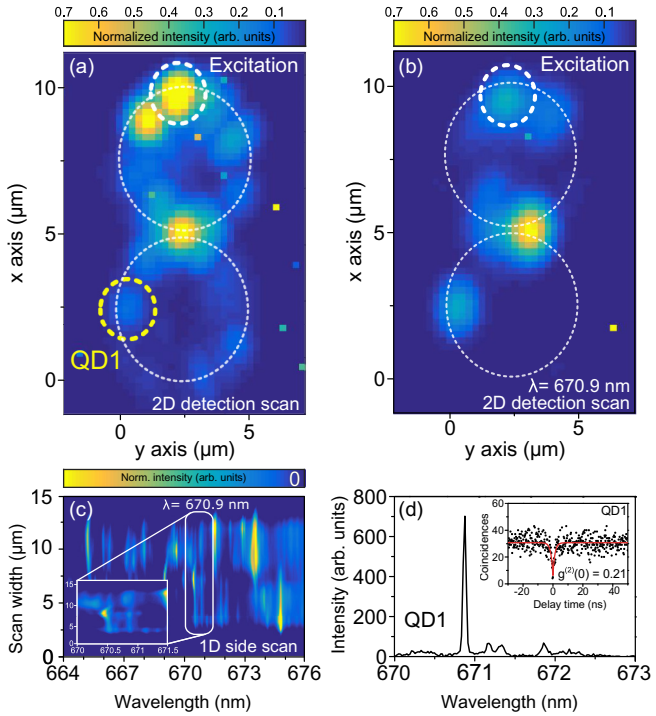

FIG. 3. (a) Color-scale plot of a two-dimensional μ-PL scan applying an excitation power of 94.5 nW with the excitation spot fixed on the upper disk of the dimer, indicated by the dotted white circle. The map shows the complete integrated intensity. A distinct mode profile can be seen from both the excited and nonexcited disk as well as possible field enhancement at the interdisk gap. The dashed circles serve as guides to the eye and indicate the disk edges. (b) Spectrally postselected intensity map at 670.9 nm of the same measurement as in (a). The nonexcited lower disk shows a bright spot indicating a single QD excited by energy transfer via a resonant mode. (c) A one-dimensional μ-PL scan from the side of the disks reveals a resonant mode at 670.9 nm responsible for the energy transfer that excites QD1. The inset shows a close up view of the coupled mode. (d) The spectrum taken at the spatial position of QD1 depicts a sharp emission line. An autocorrelation measurement on this line is shown in the inset. Note: The excitation laser is still focused on the upper disk. The antibunching dip indicates a single QD excited via a coupled microdisk mode.

The spots of high intensity seen in the real-space images in Fig. 2 can be identified as (single) QDs emitting preferentially perpendicular to the disk surface. This way individual QDs can be conveniently selected for single dot experiments.

IV. SINGLE QD COUPLED TO A RESONANT DISK MODE

For more detailed investigations of possible single dot coupling in the microdisk systems two-dimensional PL maps have been recorded applying the $4f$ setup described above. These maps contain the complete spectral information at each spatial coordinate on the disks. A resulting PL intensity map of the total integrated emission of such a x-y scan with a fixed excitation spot on the upper disk is pictured in Fig. 3(a). Several features catch the eye: The bright spot marked with the white dotted circle indicates the position of the excitation laser. The nonexcited disk is represented in the map by the WGM profile outlining the disk geometry and indicating coupling. Again, in the gap between the disks the field is strongly enhanced. A spectrally postprocessed version of this measurement is shown in Fig. 3(b) which represents the same disk pair filtered at a wavelength of 670.9 ± 0.1 nm. A high intensity spot (referred to as QD1) can be seen on the nonexcited disk leading to the assumption of a QD that is excited by radiative transfer of excitation from the excited disk to the nonexcited mediated by a resonant disk mode. The μ-PL map in Figure 3(b) does not show distinct intensity along the disk outlines which could be assigned to a resonant mode at 670.9 nm. Therefore, a one-dimensional μ-PL scan along the disk sides has been carried out. The result in Fig. 3(c) reveals an emission line at 670.9 nm which is present in both disks highlighted by the white box. Consequently, the resonant mode responsible for the energy transfer that excites QD1 can only be detected from the disk side due to the predominant radial in-plane emission characteristics and in this case low detection of mode stray light.

Without varying the position of the excitation, the emission spectrum is obtained at the location of the spot in Fig. 3(b) (QD1) and displayed in Fig. 3(d). The high intensity peak represents the emission spot seen in the map of Fig. 3(b). An autocorrelation measurement of this emission line yielded the resulting coincidence histogram depicted in Fig. 3(d). Clear antibunching behavior can be observed from the measurements with a $g^{(2)}(0)$ value of 0.21, indicating a single emitter. This is evidence of single dot excitation in the nonexcited disk mediated by mode coupling. It is necessary to point out that no exclusive dot-to-dot excitation takes place in this measurement, since the spectrum taken at the excitation spot (not shown) reveals considerable background emission and no single QD line due to a relatively high excitation power. Such a dot-to-dot interaction will be shown in the following.

V. INDICATIONS OF ON-CHIP RESONANT SCATTERING OF TWO QDS IN DIFFERENT MICRODISKS

Figure 4(a) shows the color plot of a μ-PL map filtered postselectively at a wavelength of 668.45 ± 0.2 nm. Excitation (power: 80 nW) and detection have been scanned simultaneously above the disk surface, acquiring a spectrum at every excitation spot. Several centers of bright intensity as well as a faint ring of emission indicating a mode at 668 nm can be seen in the map, tracing the outline of the disk shape as indicated by the white dotted circles. The spots of high intensity are likely to be caused by QD emission interacting with the mode and thereby indicating its presence. Two of them are highlighted by the yellow dotted circles in Fig. 4(a). These can be identified as single QDs by autocorrelation measurements [see Figs. 4(e) and 4(f)] and serve as objects of the following study. Their normalized spectra are displayed in Fig. 4(c), labeled as QD2 and QD3 according to Fig. 4(a). Each spectrum reveals two emission lines in the highlighted area [spectral filter in Figs. 4(a) and 4(b)] with the same emission wavelength, a precondition for radiative interaction. The spectral position and the linewidths can be extracted from the data using Gaussian fit functions. The lines of QD2 have a wavelength of 668.41 and 668.55 nm and linewidths of 114 and 78 pm, respectively. The two lines of QD3 are located at 668.39 and 668.52 nm with

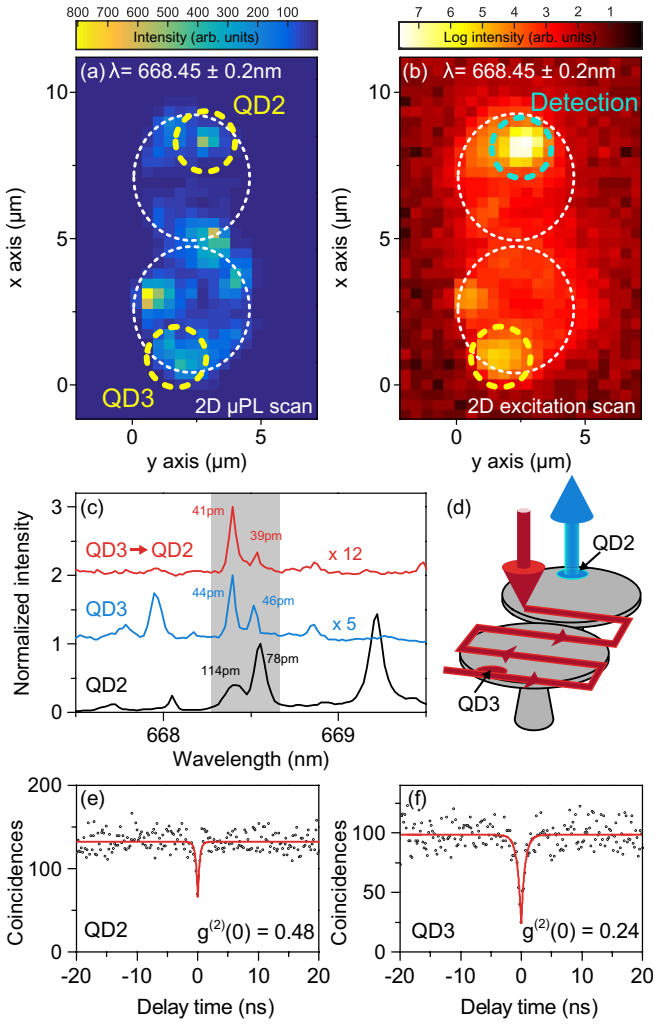

FIG. 4. (a) Normalized linear color-scale plot of a two-dimensional μ-PL scan with both excitation and detection moving across the microdisk dimer. The postselected intensity for a spectral region of 668.4 ± 0.2 nm is displayed. Two QDs with almost the same emission wavelength are found in the different disks, labeled by QD2 and QD3 [see panel (c) for their spectra]. (b) Normalized logarithmic color-scale plot of a two-dimensional (2D) excitation scan, i.e., the detection is spatially fixed on QD2 while the excitation laser is scanned across the cavity structure [see panel (d)]. We plot the intensity for the same spectral region and indicate a strong intensity increase when scanning over QD3 in the lower disk. (c) Comparison of the two ordinary μ-PL spectra for QD2 (upper disk) and QD3 (lower disk) with the spectrum recorded in the upper disk when exciting QD3 in the lower disk. The highlighted area in grey outlines the filtered spectral region in the μ-PL maps of panels (a) and (b). The inset numbers denote the full width at half maximum (FWHM) values of each peak. (e),(f) Autocorrelation measurements indicating antibunching on QD2 and QD3, respectively. Both measurements have been taken at the spectral peak on the energetically lower side of (c).

linewidths of 44 and 46 pm, respectively. The particular single lines display an energy splitting of $\approx$400 μeV and arise most probably either from different charge configurations in the QDs [31] or from a distinct fine-structure splitting of the QD exciton state [32]. In the latter case, depending on the spatial orientation of the QD in-plane dipole with respect to a TE mode, both fine-structure components can interact. Figure 4(b) displays the logarithmically plotted μ-PL map of the same disk pair, only in this instance the excitation has been scanned across the disk while the detection remained fixed to the spatial position of QD2, as schematically depicted in Fig. 4(d). The plot features again the two previously observed emission spots if compared to the μ-PL map in Fig. 4(a).

The remarkable findings of this observation is that as soon as the laser excites QD3, the collected emission at QD2 strongly increases. The corresponding spectrum is also shown in Fig. 4(c) as QD3 $\rightarrow$ QD2. Note that only the exact same lines from QD3 are detected which have a resonant counterpart at QD2. All other lines, e.g., at roughly 668 and 669.15 nm, are not observable. Most interestingly, the measured line shapes detected at QD2 when QD3 is excited (41 and 39 pm) correspond to the directly excited QD3, while they are dissimilar to the FWHM of QD2 excited on site. This could suggest that emitted photons from QD3 are transferred via a cavity mode to QD2 and are subsequently scattered by this two-level system or in other words indications of on-chip resonant scattering of quantum light from one QD by another. Differences in the intensity might occur due to different coupling strengths and scattering cross sections. The interchange of relative intensities between QD2 and QD3$\rightarrow$QD2 might appear because the mode could be slightly more centered on the energetically higher component, so a larger fraction of the left side peak would be transferred. Additionally, the higher energy peak in the on-site spectrum of QD3 displays higher intensity, so it is to be expected that a higher ratio of emission is fed into the mode and subsequently transferred, which also might cause the higher energy peak to dominate if QD2 is excited via QD3, as opposed to a direct excitation of QD3.

The coupling efficiency can be roughly estimated from the count rates. This gives an indication of the fraction of the photons that are emitted by QD3 and scattered at QD2. As indicated in Fig. 4(c) the difference in count rates is a factor of 2.4 and thus the coupling efficiency accounts to $\approx$40%. This considerable value is probably due to the high Q factor, which enhances the capture and storage of photons into the cavity modes and thus increases the likelihood of transfer into the other disk and subsequent excitation of QD2.

Note, however, a compelling proof of single-photon interaction between QD2 and QD3 would require further experiments in the form of an autocorrelation measurement on QD2 while exciting QD3, cross-correlation measurements and a reversed excitation/detection configuration on QD2 and QD3 [33].

VI. CONCLUSION

In conclusion, we have demonstrated the identification of resonant cavity modes by μ-PL scans and real-space imaging. Using such modes, the excitation of single QDs located in another disk is possible and was proved by autocorrelation measurements. Finally, we presented indications of photons emitted from one QD which are transferred to the other disk

via a resonant mode where they are resonantly scattered by another QD.

For future applications and a more detailed investigation of our basic results, we have to reinstate and further develop advanced tuning mechanisms to control the QD emission wavelength and, thus, the scattering mechanism.

ACKNOWLEDGMENTS

The authors gratefully acknowledge financial support by the Deutsche Forschungsgemeinschaft via Grant No. SFB/TRR21. We thank T.-L. Liu for processing the high quality samples.

S. Seyfferle and F. Hargart contributed equally to this work.

[1] D. Loss and D. P. DiVincenzo, Phys. Rev. A **57**, 120 (1998).

[2] S.-S. Li, J.-B. Xia, J.-L. Liu, F.-H. Yang, Z.-C. Niu, S.-L. Feng, and H.-Z. Zheng, J. Appl. Phys. **90**, 6151 (2001).

[3] A. Imamoglu, D. D. Awschalom, G. Burkard, D. P. DiVincenzo, D. Loss, M. Sherwin, and A. Small, Phys. Rev. Lett. **83**, 4204 (1999).

[4] S. Reitzenstein, A. Löffler, C. Hofmann, A. Kubanek, M. Kamp, J. P. Reithmaier, A. Forchel, V. D. Kulakovskii, L. V. Keldysh, I. V. Ponomarev, and T. L. Reinecke, Opt. Lett. **31**, 1738 (2006).

[5] A. Laucht, J. M. Villas-Bôas, S. Stobbe, N. Hauke, F. Hofbauer, G. Böhm, P. Lodahl, M.-C. Amann, M. Kaniber, and J. J. Finley, Phys. Rev. B **82**, 075305 (2010).

[6] H. Kim, D. Sridharan, T. C. Shen, G. S. Solomon, and E. Waks, Opt. Express **19**, 2589 (2011).

[7] M. Bayer, T. Gutbrod, J. P. Reithmaier, A. Forchel, T. L. Reinecke, P. A. Knipp, A. A. Dremin, and V. D. Kulakovskii, Phys. Rev. Lett. **81**, 2582 (1998).

[8] A. Dousse, J. Suffczynsk, A. Beveratos, O. Krebs, A. Lemaitre, I. Sagnes, J. Bloch, P. Voisin, and P. Senellart, Nature (London) **466**, 217 (2010).

[9] A. Majumdar, A. Rundquist, M. Bajcsy, and J. Vuckovic, Phys. Rev. B **86**, 045315 (2012).

[10] H. Lin, J.-H. Chen, S.-S. Chao, M.-C. Lo, S.-D. Lin, and W.-H. Chang, Opt. Express **18**, 23948 (2010).

[11] J. C. L. Carreño, C. Sánchez Muñoz, E. del Valle, and F. P. Laussy, Phys. Rev. A **94**, 063826 (2016).

[12] J. P. Vasco, P. S. S. Guimarães, and D. Gerace, Phys. Rev. B **90**, 155436 (2014).

[13] J. P. Vasco, D. Gerace, P. S. S. Guimarães, and M. F. Santos, Phys. Rev. B **94**, 165302 (2016).

[14] T. C. H. Liew and V. Savona, Phys. Rev. Lett. **104**, 183601 (2010).

[15] M. Bamba, A. Imamoğlu, I. Carusotto, and C. Ciuti, Phys. Rev. A **83**, 021802 (2011).

[16] D. Gerace, H. E. Tureci, A. Imamoğlu, V. Giovannetti, and R. Fazio, Nat. Phys. **5**, 281 (2009).

[17] M. J. Hartmann, F. G. S. L. Brandão, and M. B. Plenio, Nat. Phys. **2**, 849 (2006).

[18] A. D. Greentree, C. Tahan, J. H. Cole, and L. C. L. Hollenberg, Nat. Phys. **2**, 856 (2006).

[19] S. R. K. Rodriguez, A. Amo, I. Sagnes, L. Le Gratiet, E. Galopin, A. Lematre, and J. Bloch, Nat. Commun. **7**, 11887 (2016).

[20] M. Witzany, R. Roßbach, W.-M. Schulz, M. Jetter, P. Michler, T.-L. Liu, E. Hu, J. Wiersig, and F. Jahnke, Phys. Rev. B **83**, 205305 (2011).

[21] M. Benyoucef, S. Kiravittaya, Y. F. Mei, A. Rastelli, and O. G. Schmidt, Phys. Rev. B **77**, 035108 (2008).

[22] M. Witzany, T.-L. Liu, J.-B. Shim, F. Hargart, E. Koroknay, W.-M. Schulz, M. Jetter, E. Hu, J. Wiersig, and P. Michler, New J. Phys. **15**, 013060 (2013).

[23] A. Faraon and J. Vuckovic, Appl. Phys. Lett. **95**, 043102 (2009).

[24] A. Faraon, D. Englund, D. Bulla, B. Luther-Davies, B. J. Eggleton, N. Stoltz, P. Petroff, and J. Vuckovic, Appl. Phys. Lett. **92**, 043123 (2008).

[25] E. Gil-Santos, C. Baker, A. Lematre, C. Gomez, G. Leo, and I. Favero, Nat. Commun. **8**, 14267 (2017).

[26] J. P. Reithmaier, G. Sek, A. Löffler, C. Hofmann, S. Kuhn, S. Reitzenstein, L. V. Keldysh, V. D. Kulakovskii, T. L. Reinecke, and A. Forchel, Nature (London) **432**, 197 (2004).

[27] E. Peter, P. Senellart, D. Martrou, A. Lemaître, J. Hours, J. M. Gérard, and J. Bloch, Phys. Rev. Lett. **95**, 067401 (2005).

[28] K. Srinivasan, M. Borselli, O. Painter, A. Stintz, and S. Krishna, Opt. Express **14**, 1094 (2006).

[29] G. J. Beirne, M. Reischle, R. Roßbach, W.-M. Schulz, M. Jetter, J. Seebeck, P. Gartner, C. Gies, F. Jahnke, and P. Michler, Phys. Rev. B **75**, 195302 (2007).

[30] M. M. Sigalas, D. A. Fattal, R. S. Williams, S. Wang, and R. G. Beausoleil, Opt. Express **15**, 14711 (2007).

[31] M. Reischle, G. J. Beirne, W.-M. Schulz, M. Eichfelder, R. Roßbach, M. Jetter, and P. Michler, Opt. Express **16**, 12771 (2008).

[32] M. Sugisaki, H.-W. Ren, S. V. Nair, K. Nishi, S. Sugou, T. Okuno, and Y. Masumoto, Phys. Rev. B **59**, R5300 (1999).

[33] These measurements were planned but prevented due to a technical accident with the cryostat, which caused the sample to be heated up to approximately 400 K. After a renewed cooling cycle and detection of the QD2-QD3 system the resonance was found to be broken and the sample largely degraded.